Prediction of Fatigue Lives in Additively Manufactured Alloys based on the Crack-Growth Concept

Aref Yadollahi[1,2*], Mohammad J. Mahtabi[1,2], Haley R. Doude[2], and James C. Newman Jr.[3]

[1] Department of Mechanical Engineering, Mississippi State University, MS 39762
[2] Center for Advanced Vehicular Systems (CAVS), Mississippi State, MS 39762
[3] Department of Aerospace Engineering, Mississippi State University, MS 39762

Abstract

This paper aims to predict the fatigue behavior of additively manufactured alloys using crack-growth data. Among different sources of damage under cyclic loadings, fatigue due to cracks originated from voids is the most life-limiting failure mechanism in powder-based metal additive manufacturing (AM) parts. Hence, the ability to predict the fatigue behavior of AM materials based on the void features is the first step toward improving AM part reliability. Test results from the literature on AM alloys are analyzed herein to model fatigue behavior based on the semi-circular surface flaws. The fatigue-life variations in the specimens are captured using the distribution of defect size. The results indicate that knowing the statistical distribution of the defect size can provide the opportunity of predicting the scatter in the fatigue-life of the AM materials, using an appropriate fatigue analysis code.

Keywords: Additive manufacturing (AM); Laser-Powder Bed Fusion (L-PBF); Fatigue-life prediction; Crack growth; FASTRAN

1. Introduction

Additive Manufacturing (AM) refers to any technology for fabricating 3D parts based on a CAD model and through layer-by-layer addition of material [1]. Various AM techniques have been developed in the past decades, which vary in feedstock material form and method of manufacturing [2]. Powder-based metal AM has gained significant attention by commercial and academic sectors in recent years [3]. Subsequently, AM is being employed in many industries, including aerospace and biomedical engineering to fabricate customized parts with complex geometries. However, fatigue and durability of the AM parts are still two of the most important challenges in real-world applications of AM parts [4,5].

Ensuring part quality is the main challenge for additively manufacturing real structural and functional parts [5,6]. Despite the significant research efforts on the parameter optimization/control in AM process, fabricating a defect-free part with uniform microstructure has not been fully achieved yet [6–8]. Variations in the AM systems, feedstock, and building procedures cause significant distinctions and uncertainties in the mechanical properties of AM materials [5]. In addition, alteration of any of the involved parameters in the AM process, such as power setting, beam travel speed, layer thickness, etc., as well as the geometrical aspects of the part, affect the thermal histories during fabrication, and consequently, the microstructural features of the fabricated parts [4,5].

Among the different mechanical properties, failure under cyclic loading (i.e. fatigue) is a major threat for the metallic AM parts in various applications [5,9–11]. This is due to the fact that fatigue failure is a local phenomenon, thus, fatigue life is more directly affected by impurities and microstructural heterogeneity — inherent features of the current metal AM parts. In addition, not only AM materials exhibit shorter fatigue lives — compared to their wrought counterparts — their fatigue lives also display significantly greater uncertainty and scatter [4,5]. As a result, the first step toward improving AM part reliability – at least for the particular applications not requiring very long fatigue lives – is to understand and be able to model the influences of void features (e.g., size, shape, and distribution) on the fatigue behavior of AM materials.

The crack-growth concept is employed in this paper to predict the fatigue-life of AM materials. Test results from the literature on Inconel 718 fabricated via a laser-powder bed fusion (L-PBF) method and the plasticity-induced crack-closure model FASTRAN [12] are used to predict fatigue-life of specimens. Scatters in fatigue-life of this alloy are also captured based on the variations observed in the size and shape of voids.

2. Material and Testing

Inconel 718 specimens, fabricated using a laser-powder bed fusion (L-PBF) system (Concept Laser M1) at NASA's Marshall Space Flight Center (MSFC) [14], were considered in this paper for fatigue-life prediction based on the crack-growth approach. All the mechanical test results for the same material are taken from the literature [5,13,14]. All the fabricated specimens underwent intensive heat treatment schedule in the following order [13,14]: (1) stress relieving at 1065 °C for 1.5 h, followed by furnace cooling; (2) HIPing at 1165 °C and ~100 MPa for 3-4 hours; (3) solution treating at 1066 °C for 1 hour then air cooling [15]; (4) aging at 760 °C for 10 hours then furnace cooling to 650 °C and treating for total of 20 hours [15]. The microstructure was homogenized and completely recrystallized and the small porosity was healed after this heat treatment process [5,13,14].

Two different sets of round uniform stress (K_T = 1) fatigue specimen with a gage diameter of 5 mm were fabricated in near-net/net shape using the same machine [13,14]: (i) one set of specimens — called "defective build" — contained lack-of-fusion defects; (ii) the other set — referred to as "non-defective build" — were free of such defects. Fatigue specimens were tested at low stress ground (LSG) surface finish [13,14]. Constant amplitude, uniaxial high cycle fatigue (HCF) data for the defective and non-defective build sets at room temperature [5,13,14] are presented in Figure 1. All the HCF experiments were conducted under force-controlled constant-amplitude axial fatigue test condition [5,13,14], according to ASTM E466 [16]. Non-defective build specimens were tested at stress ratio ($R = \sigma_{min}/\sigma_{max}$) of 0.1, while the HCF data of defective built in LSG surface finish were obtained from fully reversed condition, i.e. R = -1 [5,13,14].

The large-crack data (i.e. ΔK-da/dN) were obtained from compact tension, C(T), specimens (W = 38.1 mm and B = 6.35 mm) [13,14]. All the data used in this paper were collected at room temperature (i.e. nominal lab conditions) [5,13,14]. The crack-growth rate data, da/dN, versus stress-intensity factor range, ΔK, were generated according to ASTM E647 [17], based on compression precracking (CPC) procedure at R = 0.1 and 0.7 are plotted in Figure 2.

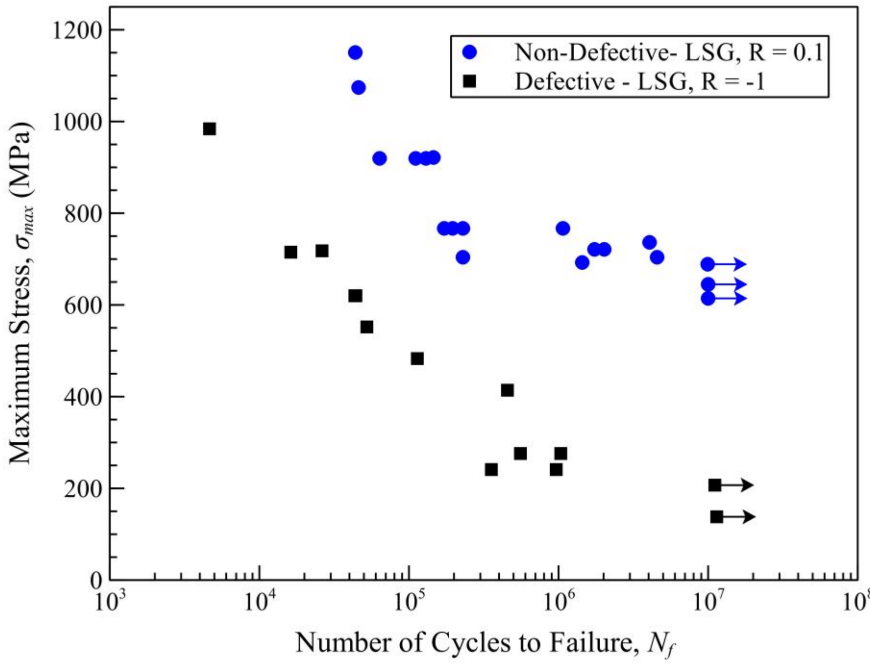

Figure 1. Experimental HCF data for L-PBF Inconel 718 fabricated in vertical (V) and horizontal (H) orientations in as-built and low stress ground (LSG) surface conditions [5,13,14].

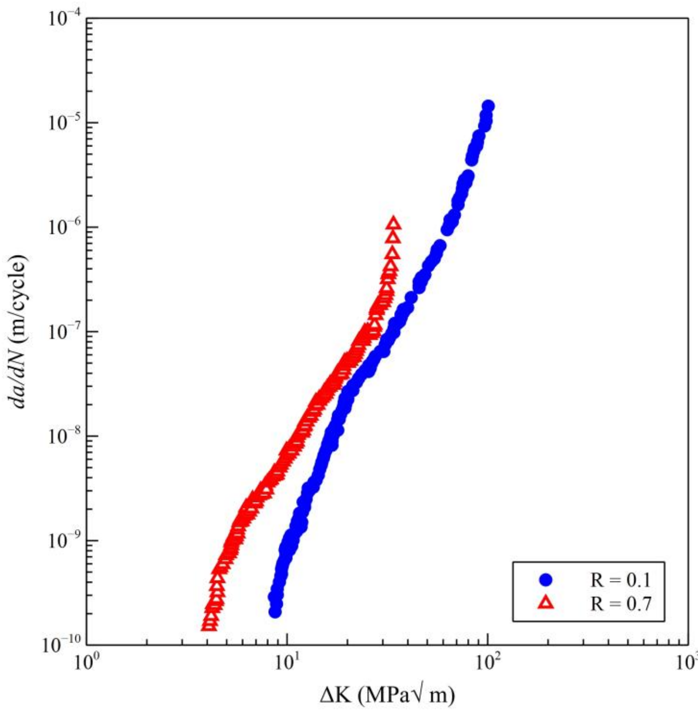

Figure 2. Experimental large crack-growth data for L-PBF Inconel 718 [13,14].

3. Fatigue-Life Prediction

In AM materials, cracks initiating from the voids located near the surface of the specimen seem to be the main life-limiting failure mechanism [9,11,18–20]. Thus, the fatigue-life prediction based on the crack-growth concept would be a promising method for AM materials, considering that the presence of process-induced voids with large size and irregular shape is inevitable in the current state of AM technique. FASTRAN code [12] was employed in this study together with two-parameter fracture criterion [21–23] to predict the fatigue life of L-PBF Inconel 718 based on the geometry of initial flaws and the fracture mechanics properties of the material. The area and aspect ratio of voids — in a plane perpendicular to the loading direction — was considered as the geometrical parameters to be used for the fatigue-life predictions. Analysis of the fatigue fracture surfaces of L-PBF Inconel 718 revealed that surface-connected voids for the LSG specimens and discontinuities on the as-built specimens' free surface serve as the crack initiation sites [4,14]. Therefore, initial cracks in this study are modelled as the semi-circular/elliptical surface flaws.

Effective stress-intensity factor, ΔK_{eff}, as a function of crack-growth rate, *da/dN*, was obtained using Newman's crack-closure model [24]. The large-crack results and the ΔK_{eff} -rate for L-PBF Inconel 718 are shown in Figure 3. In this study, the plasticity-induced closure model does not collapse the large-crack-growth threshold (ΔK-rate) data onto a unique ΔK_{eff}-rate relation in the threshold regime, thus, the high stress-ratio (R = 0.7) data were used to estimate the ΔK_{eff}-rate relation in this regime. Since in the threshold regime, the actual ΔK_{eff}-rate data would lie at lower values of ΔK_{eff} measured based on large-crack data [25], the baseline curve is chosen to be lower in this regime in the present study, to account for the small-crack effects.

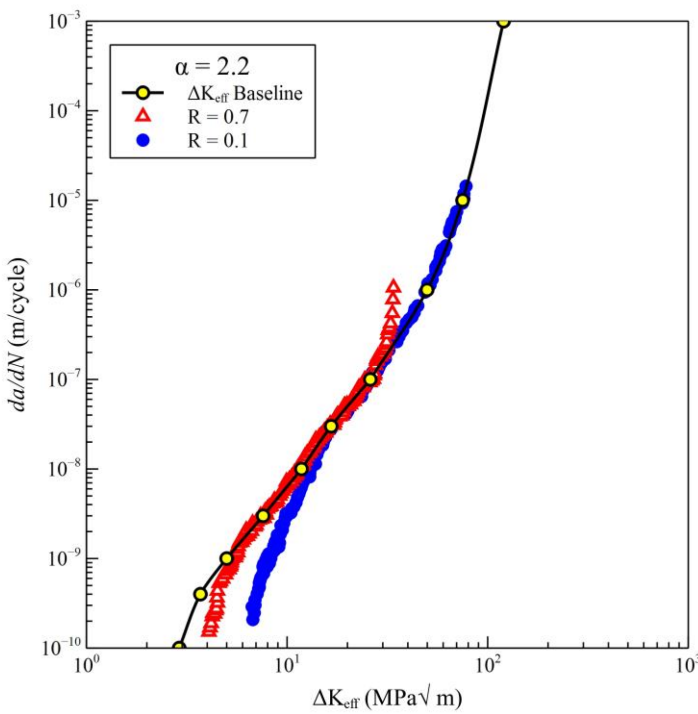

Figure 3. Effective stress-intensity factor (ΔK_{eff}) against crack-growth rate for large cracks with small-crack estimate for L-PBF Inconel 718.

4

Fatigue test results [5,13,14] and the predicted curves for defective and non-defective builds in LSG surface finish are shown in Figure 4. For the defective build, fatigue-life prediction using FASTRAN was made based on a semi-circular initial surface flaw of $a_i= c_i$=120 µm size (i.e. A.R. = $2c_i /a_i$ = 2) that had an equal surface area (in µm^2) and aspect ratio to the average values of voids, from which the fatigue cracks were initiated. As seen from Figure 5, the predicted fatigue curve for defective build agreed well with the test data using the real initial flaw size. The baseline ΔK_{eff}-rate curve in the threshold regime was found by trial-and-error to better fit the experimental fatigue data. Using the provided baseline ΔK_{eff}-rate curve, a predicted fatigue curve based on an initial flaw size of $a_i = c_i$ = 12 µm fits the non-defective test data at R = 0.1 quite well.

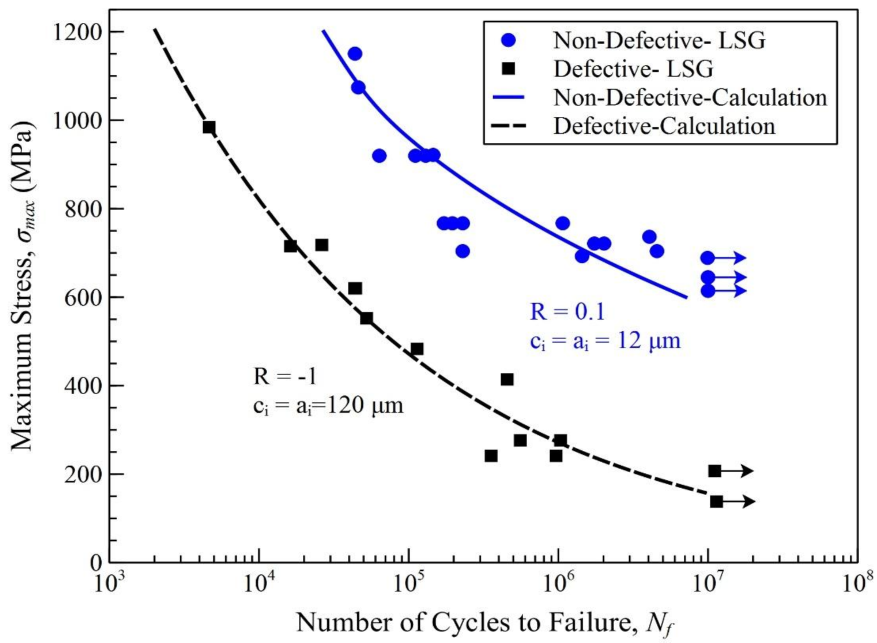

Figure 4. Experimental data [5,13,14] and predicted fatigue curves for different builds of L-PBF Inconel 718 in LSG surface condition using FASTRAN code.

3.1. Effect of defect size

A range of possible fatigue lives, depending on the initial flaw size range, can be predicted using FASTRAN code. Results for the effect of void size on the fatigue life of defective and non-defective builds are shown in Figure5. For the defective build, the aspect ratio of the initial flaw was assumed to be equal to 2 (i.e. $a_i = c_i$), corresponding to the average aspect ratio of detected voids on the fracture surface of fatigued specimens. The initial flaw sizes then were calculated based on the area of largest and smallest voids, which served as crack initiation sites. Using the range of void sizes, lower and upper bounds were determined for the fatigue data, as shown in Figure 5(a).

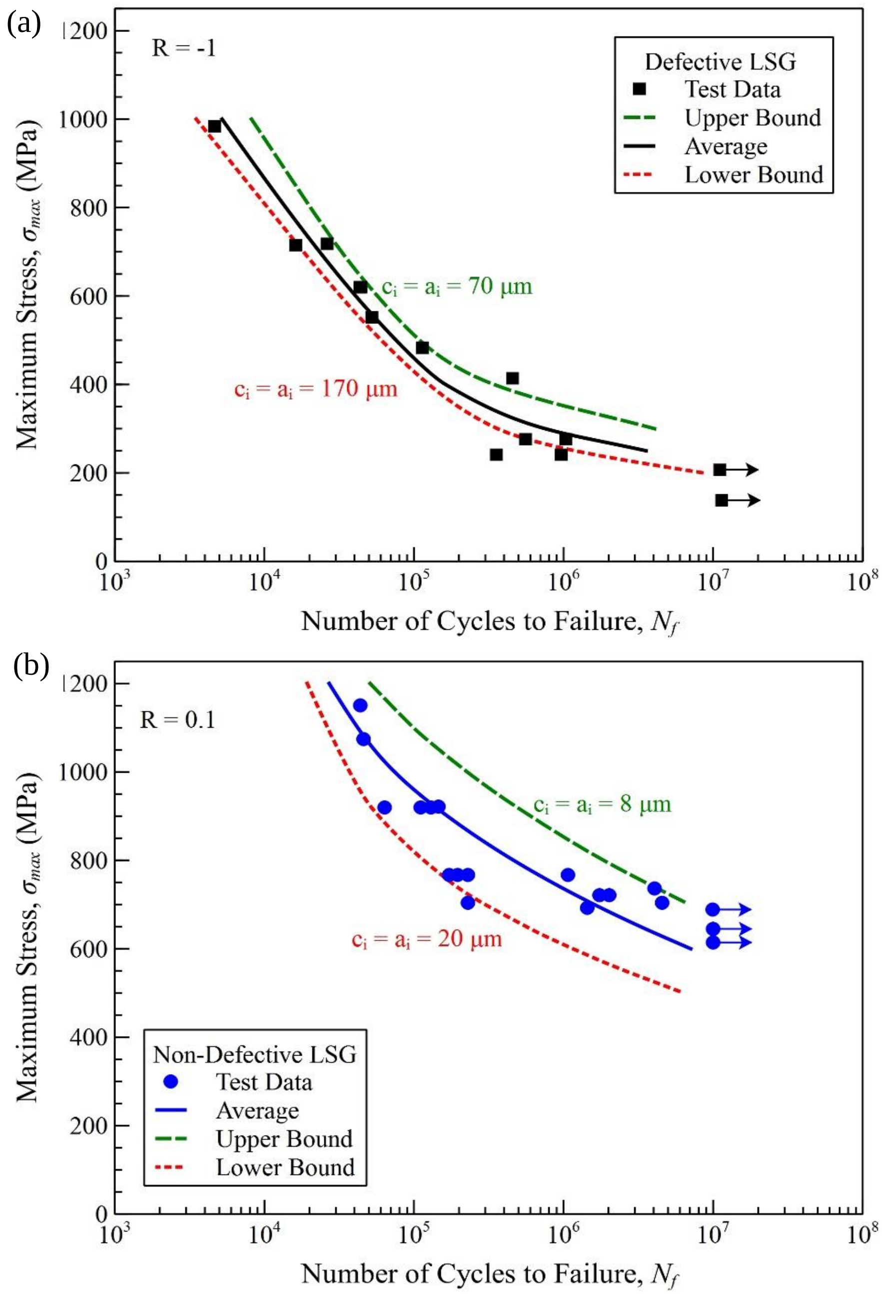

Figure 5. Effect of void size on fatigue life of (a) defective [5] and (b) non-defective [13,14] builds L-PBF Inconel 718.

For the non-defective build set, size of the initial flaws was determined by trial-and-error in a way that the predicted fatigue curves captured the scatter of fatigue-life in experimental data. As seen from Figure 5(b), the predicted upper and lower fatigue bounds fit the experimental data satisfactorily and most of the fatigue data fall within the fatigue curves for EIFSs of $a_i = c_i = 8$ μm and $a_i = c_i = 20$ μm.

3.2. Effect of defect shape

The variation of fatigue-lives with respect to the void shape (i.e. aspect ratio) was evaluated for the defective build. For this set, the total variation in void aspect ratios (A.R. = $2c_i/a_i$) was observed on the fracture surface of fatigued specimens to be from 1 to 3, with an average of 2. The results of the fatigue-life prediction using FASTRAN code for each of the crack shapes are presented in Figure 6. As seen, for AM Inconel 718, different void shapes do not lead to a significant change in the overall fatigue-lives of the defective build specimens. Results indicate that the fatigue-life of AM materials was more affected by void size as compared to void shape — at least when the crack initiation sites were located on the specimens' surface.

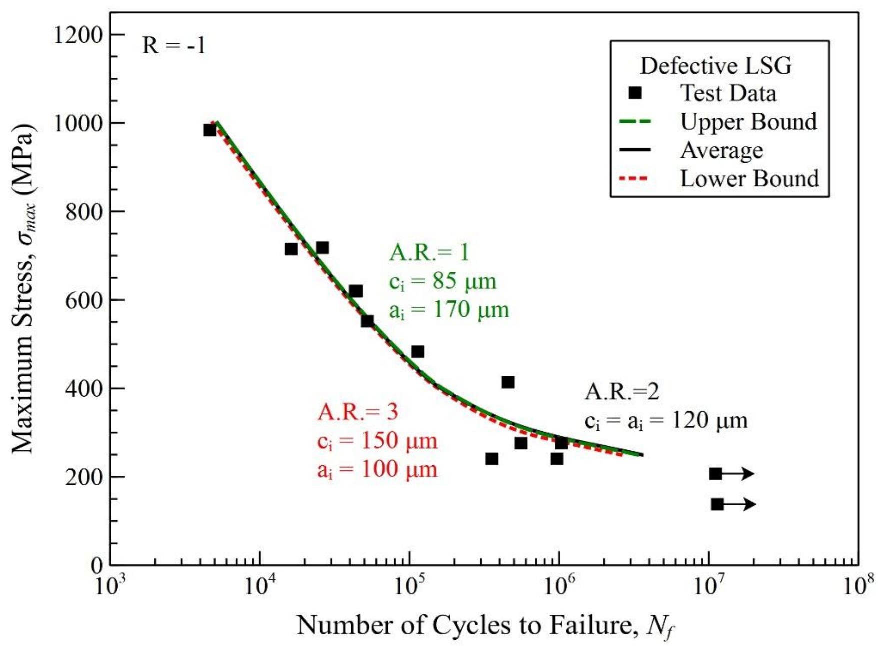

Figure 6. Effect of void shape on fatigue-life of defective build L-PBF Inconel 718 [5].

4. Conclusions

A crack-closure based fatigue-crack-growth code was used to investigate the effect of defect features, such as size and shape, on the fatigue life of Inconel 718, fabricated using an L-PBF technique. It was shown that the void size is the most influential defect feature on the fatigue-life of AM materials, at least when the crack initiation sites are observed on the specimens' surface. This implies that knowledge of the statistics of the void size, can lead to evaluation of the variations in fatigue-life of AM materials based on the crack-growth concept and crack-closure model. It was also shown that in presence of large surface flaws, the shape of the void has minimal effects on the fatigue life of AM materials.

5. References

[1] ASTM F2792-12a, Standard Terminology for Additive Manufacturing Technologies, ASTM International, West Conshohocken, PA, 2012.

[2] S.M. Thompson, L. Bian, N. Shamsaei, A. Yadollahi, An Overview of Direct Laser Deposition for Additive Manufacturing; Part I: Transport Phenomena, Modeling and Diagnostics, Addit. Manuf. 8 (2015) 36–62.

[3] T. Wohlers, 3D Printing and Additive Manufacturing State of the Industry. Annual Worldwide Progress Report, Wohlers Rep. (2016).

[4] N. Shamsaei, A. Yadollahi, L. Bian, S.M. Thompson, An Overview of Direct Laser Deposition for Additive Manufacturing; Part II: Mechanical Behavior, Process Parameter Optimization and Control, Addit. Manuf. 8 (2015) 12–35.

[5] A. Yadollahi, N. Shamsaei, Additive Manufacturing of Fatigue Resistant Materials: Challenges and Opportunities, Int. J. Fatigue. 98 (2017) 14–31.

[6] M. Seifi, M. Gorelik, J. Waller, N. Hrabe, N. Shamsaei, S. Daniewicz, J.J. Lewandowski, Progress Towards Metal Additive Manufacturing Standardization to Support Qualification and Certification, JOM. 69 (2017) 439–455.

[7] A.M. Aboutaleb, L. Bian, A. Elwany, N. Shamsaei, S.M. Thompson, G. Tapia, Accelerated Process Optimization for Laser-Based Additive Manufacturing by Leveraging Similar Prior Studies, IISE Trans. 49 (2017) 31–44.

[8] M. Khanzadeh, R.J. Marandi, M.S. Tootooni, L. Bian, B. Smith, P. Rao, Profiling and Optimizing the Geometric Accuracy of Additively Manufactured Components via Self-Organizing Map, in: Proc. 26th Annu. Int. Solid Free. Fabr. Symp. – Addit. Manuf. Conf., 2016.

[9] M.J. Mahtabi, N. Shamsaei, M.R. Mitchell, Fatigue of Nitinol: The State-of-the-Art and Ongoing Challenges, J. Mech. Behav. Biomed. Mater. 50 (2015) 228–254.

[10] R.I. Stephens, A. Fatemi, R.R. Stephens, H.O. Fuchs, Metal Fatigue in Engineering, Second, Wiley, 2000.

[11] A. Yadollahi, N. Shamsaei, S.M. Thompson, A. Elwany, L. Bian, Effects of Building Orientation and Heat Treatment on Fatigue Behavior of Selective Laser Melted 17-4 PH Stainless Steel, Int. J. Fatigue. (2016).

[12] J.C. Newman Jr., FASTRAN-2: A Fatigue Crack Growth Structural Analysis Program, NASA STIRecon Tech. Rep. N. 92 (1992).

[13] N. Barbosa, NIST/ASTM Workshop on Fatigue and Fracture in Additively Manufactured Materials, (2016).

[14] D. Wells, Overview of Fatigue and Damage Tolerance Performance of Powder Bed Fusion Alloy N07718, (2016).

[15] SAE AMS 5664, Nickel Alloy, Corrosion and Heat Resistant, Bars, Forgings, and Rings, SAE International, 2006.

[16] ASTM E466-07, Practice for Conducting Force Controlled Constant Amplitude Axial Fatigue Tests of Metallic Materials, ASTM International, West Conshohocken, PA, 2007.

[17] ASTM E647, Standard Test Method for Measurement of Fatigue Crack Growth Rates, ASTM International, West Conshohocken, PA, 2015.

[18] A. Bagheri, M.J. Mahtabi, N. Shamsaei, Fatigue Behavior and Cyclic Deformation of

Additive Manufactured NiTi, J. Mater. Process. Technol. (2017).
[19] S. Leuders, M. Vollmer, F. Brenne, T. Tröster, T. Niendorf, Fatigue Strength Prediction for Titanium Alloy TiAl6V4 Manufactured by Selective Laser Melting, Metall. Mater. Trans. A. 46 (2015) 3816–3823.
[20] E. Wycisk, A. Solbach, S. Siddique, D. Herzog, F. Walther, C. Emmelmann, Effects of Defects in Laser Additive Manufactured Ti-6Al-4V on Fatigue Properties. Phys Procedia 2014;56:371–8.
[21] M.J. Mahtabi, A. Sanford, N. Shamsaei, J.C. Newman, Transferability of the Two-Parameter Fracture Criterion for 2219 Aluminium alloy cracked configurations, Fatigue Fract. Eng. Mater. Struct. 39 (2016) 335–345.
[22] J.C. Newman, Fracture Analysis of Surface- and Through-Cracked Sheets and Plates, Eng. Fract. Mech. 5 (1973) 667–689.
[23] J.C. Newman, M.J. Mahtabi, Improved Two-Parameter Fracture Criterion for Various Crack Configurations under Tension and Bending Loads, in: ASTM International, Toronto, Canada, 2017.
[24] J.C. Newman, A Crack-Closure Model for Predicting Fatigue Crack Growth under Aircraft Spectrum Loading, in: Methods Models Predict. Fatigue Crack Growth Random Load, ASTM International, 1981.
[25] J.C. Newman, E.P. Phillips, M.H. Swain, Fatigue-Life Prediction Methodology using Small-Crack Theory, Int. J. Fatigue. 21 (1999) 109–119.